

# Early Monitoring of Exotic Mangrove *Sonneratia* in Hong Kong Using Deep Convolutional Network at Half-Meter Resolution

Luoma Wan<sup>ID</sup>, Hongsheng Zhang<sup>ID</sup>, Member, IEEE, Mingfeng Liu<sup>ID</sup>, Yinyi Lin<sup>ID</sup>, Student Member, IEEE, and Hui Lin, Senior Member, IEEE

**Abstract**—*Sonneratia* have posed a threat to native mangrove species in Hong Kong. Early detection of individual *Sonneratia* when they are introduced and naturalized before invasion is essential for native mangrove species protection, especially for *Sonneratia* with a strong ability of propagation. This letter aims to provide an effective way to the accurate detection of individual *Sonneratia*. Specifically, using very high spatial resolution remotely sensed data, we adapt the RetinaNet, incorporating multiscale features for sapling detection and convolutional neural networks for detecting the *Sonneratia* distributed scatteredly among native species. The *Sonneratia* were detected with a higher mean average precision (mAP) 0.50 of 0.3891 with a precision of 0.5465 than that from the deformable part model. In addition, 3678 *Sonneratia* were detected at early stage. This letter can support the government for mangrove forest management and offer a scientific guidance for adequate response to the species invasion, like annual removal of *Sonneratia*, and then reduce the consumption of labor and time over a large scale. In addition, it can provide a quantitative survey for *Sonneratia* management.

**Index Terms**—Deep learning, invasion detection, Mai Po, mangrove, *Sonneratia*.

## I. INTRODUCTION

MANGROVE, one of the most productive systems in the tropical and subtropical regions, provides essential bioecological services, biodiversity protection, carbon sequestration, and economic benefits [1]. During the past decades, mangrove forests have suffered from great loss due to human activities [2]. To restore mangrove forests, the exotic species with highly adaptive capacity of environment were introduced [3]. Recently, the concern on the effect of introduced

Manuscript received May 7, 2019; revised October 31, 2019; accepted January 22, 2020. Date of publication February 10, 2020; date of current version January 21, 2021. This work was supported in part by the Research Grants Council (RGC) under Grant HKU 14605917 and Grant HKU 14635916, in part by the National Natural Science Foundation of China under Grant 41401370 and Grant 41671378, and in part by the Seed Fund for Basic Research for New Staff under Grant 201909185015. (Corresponding author: Hongsheng Zhang.)

Luoma Wan, Mingfeng Liu, and Yinyi Lin are with the Institute of Space and Earth Information Science, The Chinese University of Hong Kong, Hong Kong (e-mail: romal@link.cuhk.edu.hk; mingfengliu@link.cuhk.edu.hk; yinyilin@link.cuhk.edu.hk).

Hongsheng Zhang is with the Department of Geography, The University of Hong Kong, Hong Kong (e-mail: zhanghs@hku.hk).

Hui Lin is with the Key Lab of Poyang Lake Wetland and Water-shed Research of Ministry of Education, School of Geography and Environment, Jiangxi Normal University, Nanchang 330022, China (e-mail: huulin@cuhk.edu.hk).

Color versions of one or more of the figures in this letter are available online at <https://ieeexplore.ieee.org>.

Digital Object Identifier 10.1109/LGRS.2020.2969522

species to domestic ecosystem beyond the mangrove area loss arises [4].

Exotic species invasion is a serious ecological problem, since it will alter the nutrient cycling, hydrology, energy budgets, and biodiversity balance of the native ecosystem [5]–[7]. *Sonneratia caseolaris* were originally introduced from Hainan to reconstruct mangrove forests in the Futian National Nature Reserve of Shenzhen, but they have been viewed as an invader [8] and annually removed by the Agriculture, Fisheries, and Conservation Department (AFCD) due to the threat of highly adaptive capacity of environment. In general, the invasion process includes three steps: introduction, naturalization, and invasion [9]. Early detection and rapid response are effective to control invasion, and the efforts enormously rely on early detection. *Sonneratia*, at the early stage of invasion, tend to be saplings and individuals distributed in mudflat or among native species. They, therefore, are primarily cut off with low labor cost to control invasion. However, for *Sonneratia* that have formed a community, AFCD is apt to keep them, since the effect of the significant disturbance on native species is uncertain. As a result, we target individual *Sonneratia* including saplings. Nevertheless, early detection of them from dense mangrove forests over a large scale is still a challenge, blocking quick response to invasion. Therefore, an effective approach for early detection and scientific control is urgent.

## II. RELATED WORKS

Compared with the tasks of mangrove species mapping [10], individual *Sonneratia* detection will provide more detailed object information rather than the area or spatial distribution derived from the classification, such as accurate location, object number, and size. In addition, this information is very important for quick and scientific response. In general, it requires very high spatial resolution (VHR) images (around 1 m) for individual tree detection [9], [11], [12]. In the low and median spatial resolution images, the early signal of some individual invader will be lost or hard to be detected. The approaches using an optical remote sensing image for object detection consist of template matching-based, knowledge-based, object-based image analysis (OBIA)-based, and machine learning-based, which is detailedly discussed in [13]. From the survey, most of the tasks focus on the artificial objects with clear features of edges and shapes, like

buildings, roads, ships, and so on. Although some works on invasive species detection have been done [14], [15], they focused on areal extent, which may be too late for quick response, since they have formed communities [16]. Beyond that, only a few work of individual tree detection can be found. Malek *et al.* [17] adapted scale invariant feature transform (SIFT) for key points and a local binary pattern for palm detection on the unmanned aerial vehicle (UAV) image with a spatial resolution of 3.5 cm. Hung *et al.* [18] leveraged the shadow to construct the template for tree-crown detection on the UAV images with a resolution of 20 cm. However, they are with monotonous background and no high overlap. Differently, individual *Sonneratia* detection from mangrove forests is more complex due to the following challenges.

- 1) Spectral similarity among different mangrove species makes it difficult to identify one species from other [15].
- 2) Although the detailed spatial information can help in mapping mangrove species [2], [19], the interclass variability will be also magnified to affect individual *Sonneratia* detection, especially with the complex background of open mudflat or other native species and overlap.
- 3) Low intraclass variability from a similar spectrum and high interclass variability from VHR challenge the pixel-based methods in individual *Sonneratia* capture and the Object-based methods in overlapped *Sonneratia* separation.

To obtain individual mangrove, the vertical information from UAV light detection and ranging (LiDAR) was also used to avoid the aforementioned difficulties [20]. However, the low latitude of the UAV is limited in the Mai Po Nature Reserve to protect the migratory birds, and the territorial boundaries require verbose permission. Inspired by the successful applications in object detection using remote sensing with deep learning [21], the ability of abstract feature representation from deep learning was first adapted to the individual mangrove of *Sonneratia* detection, avoiding handcrafted features and the prior knowledge in [18] and [17]. This letter is expected to offer accurate location for quick response like efficient removal. The number and crow size provide quantitative surveys for better understanding of their propagation pattern, making contribution to the management of mangrove forests.

### III. STUDY SITES AND DATA SET

#### A. Study Site

The Mai Po Marshes Nature Reserve (MPMNR, Fig. 1) ( $113^{\circ}59'E$ – $114^{\circ}3'E$ ,  $22^{\circ}28'N$ – $22^{\circ}32'N$ ) located in the northwest of the New Territories, on the shores of Deep Bay, keeps the majority of mangrove forest in Hong Kong. It has been well protected since 1995 when it was named “Wetland of International importance” under the prestigious Ramsar Convention because of significant ecological service provision.

Eight species of mangroves have been reported in this area (AFCD 2015). Apart from the domestic species, *Sonneratia apetala* and *Sonneratia caseolaris* float into the reserve from the Futian National Nature Reserve of Shenzhen. They were first found on the exposed mudflat closed to the mouth of the Shenzhen river in 2000 and were found among the native

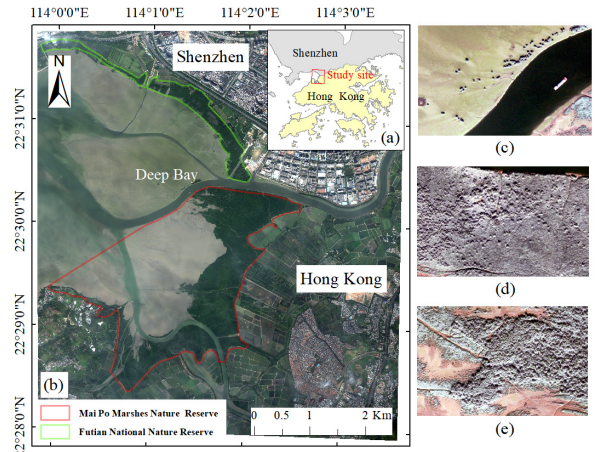


Fig. 1. (a) Study site and (b) WorldView 2 true color image, from which three patterns of *Sonneratia* distribution (c) exposed on the mudflat, (d) distributed among other native species, and (e) formed a *Sonneratia* community were observed.

species along the downstream of the Kam Tin Main Drainage Channel (MDC) in 2001 [22]. Due to the high adaptability and threat of potential colonization, these two species are viewed as invasive species and have been consistently removed by the government of Hong Kong (AFCD) since 2001 [23]–[25].

#### B. Remotely Sensed Data and Samples

A WorldView 2 image (level 2) was acquired on November 14, 2010. It was delivered with basic preprocessing including radiation correction, geometrical reference, and orthorectification, resulting in eight resampled multispectral bands and a panchromatic band with a spatial resolution of 2 and 0.5 m [Fig. 1(b)]. Using the Gram–Schmidt spectral sharpening [12], the spatial resolution of multispectral bands was improved to be the same as the panchromatic band for *Sonneratia* detection.

Due to the time gap between image acquisition and sample collection, we conducted two field surveys to recognize *Sonneratia* including potential location and features rather than collecting “real time” data. One survey was conducted along with the floating bridge in the Mai Po Nature Reserve on November 10, 2015. The other was to observe the *Sonneratia* in the estuary of the Shenzhen river from the observatory in the Futian Nature Reserve, Shenzhen, on April 11, 2017. Being faster growing, *Sonneratia caseolaris* and *Sonneratia apetala* can grow up to 15 and 20 m, respectively [22]. Therefore, they could be easily recognized among other planted mangroves by their height [22]. From the remotely sensed image, three patterns of *Sonneratia* distribution can be observed. Many *Sonneratia* saplings spread on exposed mudflat [Fig. 1(c)], many have intruded into native species [Fig. 1(d)], and many have established a new range and formed a community [Fig. 1(e)]. Since this letter aims to detect *Sonneratia* who stays at the first stage, the first two patterns will be explored.

The entire image was first cropped into image patches with a size of  $64 \times 64$  pixels, among which 329 patches containing *Sonneratia* were picked up to be samples and the individual *Sonneratia* were manually delineated (Fig. 2). The support from the Futian Nature Reserve and World Wildlife

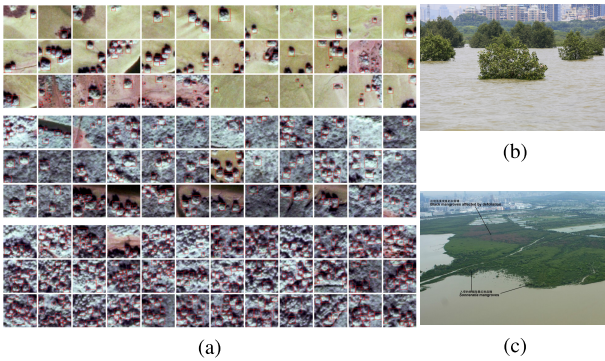


Fig. 2. Part of the samples cropped from the entire scene, and the *Sonneratia* (a) were delineated with red boxes, (b) were the *Sonneratia* in the estuary of the Shenzhen river (provided by the Futian Nature Reserve), and (c) were the *Sonneratia* intruding into Mai Po along the outmost of mangrove forests in 2012 (Source: [https://www.wwf.org.hk/news/press\\_release/?uNewsID=7220#](https://www.wwf.org.hk/news/press_release/?uNewsID=7220#)).

Fund (WWF) as well as government reports helps us with correct delineation. Notably, the image patches of pattern 3 (in rows 7–9) were also added for sample augmentation, but only those taller *Sonneratia* with the feature of protrusion similar to pattern 2 were outlined. Finally, 80% of the patches were randomly selected for training and the rest (66 patches) are for testing.

#### IV. METHODS

##### A. Feature Pyramid Extraction

Convolutional neural networks (ConvNets), such as VGG, DenseNet, and ResNet [26], are usually used for feature extraction due to outstanding performance. Considering that ResNet can construct a deeper network for high-level feature extraction by overcoming the vanishing gradients through shortcuts and train a better model with less training parameters, which lowers the demand for enormous samples, it was used in this letter. The details of ResNet can be found in [26]. *Sonneratia* at the early stage of invasion include saplings and many individual mature trees. Therefore, multiscale features for them are necessary. Feature pyramid networks (FPNs) adapting the inherent structure of feature hierarchy in ConvNets were for multiscale features via feature pyramid construction [27]. In addition, the fusion of low-level features and high-level features aims to generate a feature pyramid with multilevel features to enhance feature representation. Another metric to integrate the low-level feature map is to make up the location information loss at high-level feature maps due to the pooling layers and provide high-resolution feature map for accurate locating.

##### B. Anchor and Focal Loss

Features are for *Sonneratia* identification, while anchors are for *Sonneratia* location. Initial boxes, in general, are first proposed, and exclusion as well as adjustment were conducted to obtain the final box [28]–[30]. Rather than the sliding windows in conventional methods, a region proposal network (RPN) [7] adapts the preset anchors of three different sizes with three aspect ratios to form a translation-invariant anchor

box for each feature map at different levels. Due to high-quality region proposal with nearly cost-free in time, an RPN is widely used for the object-detection task [28], [31].

RetinaNet is a unified platform for object detection consisting of a flexible backbone of feature extractor and a task-specific classifier as well as a regressor [31]. Apart from the adaption of FPN and RPN similar to the latest methods of object detection [32], RetinaNet proposed a new loss to keep balance of positive/negative examples, and then improve the accuracy of object detection

$$FL(p_t) = -\alpha_t(1 - p_t)^\gamma \log p_t$$

$$p_t = \begin{cases} p, & y = 1 \\ 1 - p, & \text{otherwise} \end{cases} \quad (1)$$

where  $y \in \{\pm 1\}$  is the class for the ground truth and  $p \in [0, 1]$  is the model's estimated probability for positive samples with a class of 1.  $\gamma$  can modulate the cross-entropy loss, while  $\alpha_t$  is used to balance the focal loss. Finally, the focal loss makes the training focus on hard samples rather than simple negative samples and improves the object accuracy, which is useful for small-object detection from large images. In addition, the invaders of *Sonneratia* present similar scenarios of individual ones over the expansive mudflat or domestic mangrove forests.

##### C. Accuracy Assessment

Mean average precision (mAP) is a metric widely used for detection by calculating the area under the curve (AUC) of the Precision  $\times$  Recall curve [33]–[35]. Precision is given by the ratio of true-positive (TP) detections to all the detections, while recall is defined as the ratio of TP to the ground-truth instances. To calculate the area, an 11-point interpolation was adapted by sampling at 11 uniformly spaced values of recall [33], [36]. In addition, the higher mAP indicates better performance. Moreover, the value of the intersection over union (IoU) filters out the detections with lower overlapping with the ground-truth instance and then affect the mAP. Therefore, mAP with an IoU of 50% (mAP<sub>0.50</sub>), in general, was used to evaluate the performance of the detector [31]

$$\text{Precision} = \frac{\text{TP}}{\text{TP} + \text{FP}}, \quad \text{Recall} = \frac{\text{TP}}{\text{TP} + \text{FN}} \quad (2)$$

$$\text{AP} = \frac{1}{11} \sum_{r \in \{0, 0.1, \dots, 1\}} \rho_{\text{interp}}(r). \quad (3)$$

#### V. RESULTS

For training, ResNet50 was used to be the backbone with a learning rate of 1 e-5 and epochs of 50. The size of the anchor was set as {32, 64, 128, 256, 512} with the ratios of {2<sup>-1</sup>, 2<sup>0</sup>, 2<sup>1</sup>} and the scales of {2<sup>0</sup>, 2<sup>1/2</sup>, 2<sup>2/3</sup>

To evaluate the performance of RetinaNet in *Sonneratia* detection at early stage, a deformable part model (DPM),

TABLE I

ACCURACY COMPARISON BETWEEN DPM AND RETINANET; 1, 2, AND 3 MEAN THREE DIFFERENT PATTERNS THAT CAN BE FOUND FIG.2

	$mAP_{0.5}$	precision	recall
DPM	0.30626	0.3139	0.5371
RetinaNet	<b>0.38910</b>	<b>0.5465</b>	<b>0.5137</b>
DPM <sup>1</sup>	<b>0.46821</b>	0.5510	0.5870
RetinaNet <sup>1</sup>	0.45360	<b>0.6279</b>	<b>0.5745</b>
DPM <sup>2</sup>	0.31417	0.3527	0.5549
RetinaNet <sup>2</sup>	<b>0.44360</b>	<b>0.6397</b>	<b>0.5273</b>
DPM <sup>3</sup>	0.25225	0.2397	0.5000
RetinaNet <sup>3</sup>	<b>0.32030</b>	<b>0.4485</b>	<b>0.4805</b>

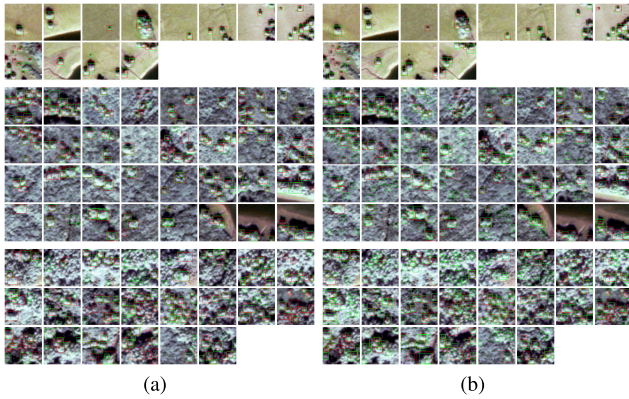


Fig. 3. *Sonneratia* detection by (a) RetinaNet and (b) DPM; the ground-truth *Sonneratia* were outlined with red boxes, while those detected are in green boxes.

a classic approach for object detection, was used for comparison, which has been successfully applied to the PASCAL visual object classes (VOC) challenge data sets [37]. To fit the requirement of input image size for the DPM, all the image patches were first downsampled to the size of  $768 \times 768$  pixels before being fed into the two models for training and testing. The indicators of  $mAP_{0.5}$ , precision, and recall were calculated for accuracy assessment (Table I). Compared with the DPM with an  $mAP_{0.5}$  of 0.30626, RetinaNet gets a higher  $mAP_{0.5}$  of 0.3891. The higher precision and lower recall mean that RetinaNet can detect more *Sonneratia* correctly with a lower rate of false alarm. Specifically, we also evaluate the model on three patterns separately. Moreover, the results show that RetinaNet obtains higher  $mAP_{0.5}$  and precision with low recall except on pattern 1, where the  $mAP_{0.5}$  that resulted from RetinaNet shows a slim decrease of 0.01461. Fig. 3 demonstrates the results of *Sonneratia* detection by two models on the testing samples. The image patches in the first two rows show that both of them can detect individual *Sonneratia* spreading in the mudflat well, but some *Sonneratia* saplings missed by DPM were also identified by RetinaNet (the third image patch in row 1 and the first image patch in row 2). For those individual *Sonneratia* who have intruded into domestic species (pattern 2), the background with similar spectral features makes DPM confused and produce more false alarms (more green boxes), while for the crowded *Sonneratia* community, instead of those protruding *Sonneratia*, more extra *Sonneratia* were detected by the DPM, since it focuses on template matching. This situation can also explain the reason for more false alarms from the DPM.

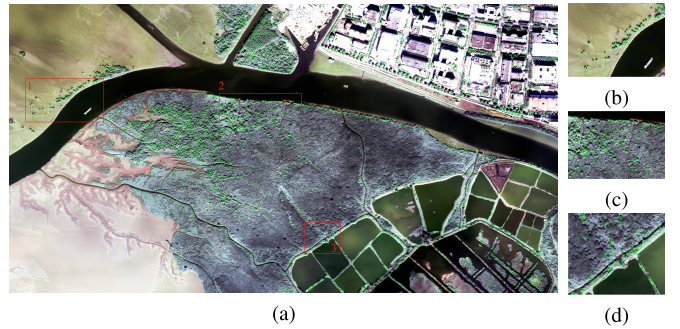


Fig. 4. (a) Detection of *Sonneratia* over the northern part of Mai Po using RetinaNet. (b)–(d) Details of three parts.

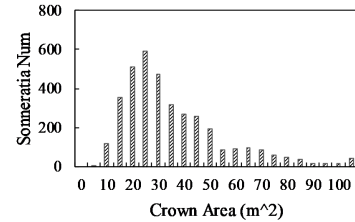


Fig. 5. Crown size of *Sonneratia* detected by RetinaNet in study site.

For the *Sonneratia* detection over the entire image, the cropped image patches with a size of  $64 \times 64$  pixels were first obtained and fed into model to get the final result after being resized [Fig. 4(a)]. The *Sonneratia* detected by RetinaNet are consistent with the mapping result in [1]. Specifically, the *Sonneratia* on the open mudflat along the Shenzhen river [Fig. 4(b)], the *Sonneratia* distributed on the opposite site of the Futian Nature Reserve [Fig. 4(c)], and the *Sonneratia* on the outmost of the Mai Po Reserve [Fig. 4(d)] can be well detected. And those have formed a community were automatically suppressed; it makes us focus on the early detection of *Sonneratia* for early warning and quick response.

## VI. DISCUSSION AND CONCLUSION

Early warning is better than postentry control for invasion management. Different from the mapping invader that is only observed after forming a community, this letter focuses on individual *Sonneratia* before forming a community for early warning. RetinaNet shows higher precision with a lower false alarm than the DPM in individual *Sonneratia* detection. The false alarms of trees along the road indicate that the extra information apart from contextual information is necessary for improvement in the future, but these false alarms can be eliminated by masking mangrove forests in advance. In this way, we finally obtained 3678 *Sonneratia* as well as their crown size Fig. 5. Most of the *Sonneratia* are with a crown area of 20–25  $m^2$ , but the result is overestimated due to shadow inclusion. Moreover, early detection of *Sonneratia* still needs support from high temporal VHR images, but it will be not a problem as with the development in sensors and data share.

## ACKNOWLEDGMENT

The authors would like to thank the editor and two anonymous reviewers for their critical comments and suggestions to improve the original letter.

## REFERENCES

- [1] L. Wan, H. Zhang, T. Wang, G. Li, and H. Lin, "Mangrove species discrimination from very high resolution imagery using Gaussian Markov random field model," *Wetlands*, vol. 38, no. 5, pp. 861–874, Oct. 2018, doi: [10.1007/s13157-017-0925-1](https://doi.org/10.1007/s13157-017-0925-1).
- [2] T. Wang, H. Zhang, H. Lin, and C. Fang, "Textural-spectral feature-based species classification of mangroves in Mai po nature reserve from worldview-3 imagery," *Remote Sens.*, vol. 8, no. 1, p. 24, Jan. 2016.
- [3] Y. Peng *et al.*, "Virtual increase or latent loss? A reassessment of mangrove populations and their conservation in Guangdong, Southern China," *Marine Pollut. Bull.*, vol. 109, no. 2, pp. 691–699, Aug. 2016.
- [4] S. Y. Lee, S. Hamilton, E. B. Barbier, J. Primavera, and R. R. Lewis, "Better restoration policies are needed to conserve mangrove ecosystems," *Nature Ecol. Evol.*, vol. 3, no. 6, pp. 870–872, Jun. 2019, doi: [10.1038/s41559-019-0861-y](https://doi.org/10.1038/s41559-019-0861-y).
- [5] R. N. Mack, D. Simberloff, W. M. Lonsdale, H. Evans, M. Clout, and F. A. Bazzaz, "Biotic invasions: Causes, epidemiology, global consequences, and control," *Ecol. Appl.*, vol. 10, no. 3, pp. 689–710, Jun. 2000.
- [6] F.-L. Li *et al.*, "Does energetic cost for leaf construction in Sonneratia change after introduce to another mangrove wetland and differ from native mangrove plants in South China?" *Mar. Pollut. Bull.*, vol. 124, no. 2, pp. 1071–1077, Nov. 2017.
- [7] D. Arán, J. GarcíAa-Duro, O. Reyes, and M. Casal, "Fire and invasive species: Modifications in the germination potential of *Acacia melanoxylon*, *Conyza canadensis* and *Eucalyptus globulus*," *Forest Ecol. Manage.*, vol. 302, pp. 7–13, Aug. 2013.
- [8] E. Bureau. (2016). *Hong Kong Biodiversity Strategy Action Plan 2016–2021*. [Online]. Available: [http://www.afcd.gov.hk/english/conservation/Con\\_hkbsap/files/HKBSAP\\_ENG\\_2.pdf](http://www.afcd.gov.hk/english/conservation/Con_hkbsap/files/HKBSAP_ENG_2.pdf)
- [9] A. Gil, A. Lobo, M. Abadi, L. Silva, and H. Calado, "Mapping invasive woody plants in Azores Protected Areas by using very high-resolution multispectral imagery," *Eur. J. Remote Sens.*, vol. 46, no. 1, pp. 289–304, Jan. 2013.
- [10] H. Zhang *et al.*, "Potential of combining optical and dual polarimetric SAR data for improving mangrove species discrimination using rotation forest," *Remote Sens.*, vol. 10, no. 3, p. 467, Mar. 2018. [Online]. Available: <https://www.mdpi.com/2072-4292/10/3/467>
- [11] M. Kamal, S. Phinn, and K. Johansen, "Object-based approach for multi-scale mangrove composition mapping using multi-resolution image datasets," *Remote Sens.*, vol. 7, no. 4, pp. 4753–4783, Apr. 2015. [Online]. Available: <https://www.mdpi.com/2072-4292/7/4/4753>
- [12] M. Liu *et al.*, "Monitoring the invasion of *spartina alterniflora* using multi-source high-resolution imagery in the Zhangjiang Estuary, China," *Remote Sens.*, vol. 9, no. 6, p. 539, May 2017. [Online]. Available: <http://www.mdpi.com/2072-4292/9/6/539>
- [13] G. Cheng and J. Han, "A survey on object detection in optical remote sensing images," *ISPRS J. Photogram. Remote Sens.*, vol. 117, pp. 11–28, Jul. 2016.
- [14] S. J. Walsh *et al.*, "QuickBird and hyperion data analysis of an invasive plant species in the Galapagos Islands of Ecuador: Implications for control and land use management," *Remote Sens. Environ.*, vol. 112, no. 5, pp. 1927–1941, May 2008. [Online]. Available: <http://www.sciencedirect.com/science/article/pii/S0034425708000205>
- [15] B. W. Heumann, "An object-based classification of mangroves using a hybrid decision tree—Support vector machine approach," *Remote Sens.*, vol. 3, no. 11, pp. 2440–2460, Nov. 2011.
- [16] F.-M. Martin, J. Müllerová, L. Borgniet, F. Dommanget, V. Breton, and A. Etvette, "Using single- and multi-date UAV and satellite imagery to accurately monitor invasive knotweed species," *Remote Sens.*, vol. 10, no. 10, p. 1662, Oct. 2018.
- [17] S. Malek, Y. Bazi, N. Alajlan, H. Alhichri, and F. Melgani, "Efficient framework for palm tree detection in UAV images," *IEEE J. Sel. Topics Appl. Earth Observ. Remote Sens.*, vol. 7, no. 12, pp. 4692–4703, Dec. 2014.
- [18] C. Hung, M. Bryson, and S. Sukkarieh, "Multi-class predictive template for tree crown detection," *ISPRS J. Photogram. Remote Sens.*, vol. 68, pp. 170–183, Mar. 2012. [Online]. Available: <http://www.sciencedirect.com/science/article/pii/S0924271612000366>
- [19] X. Huang, L. Zhang, and L. Wang, "Evaluation of morphological texture features for mangrove forest mapping and species discrimination using multispectral IKONOS imagery," *IEEE Geosci. Remote Sens. Lett.*, vol. 6, no. 3, pp. 393–397, Jul. 2009.
- [20] D. Yin and L. Wang, "Individual mangrove tree measurement using UAV-based LiDAR data: Possibilities and challenges," *Remote Sens. Environ.*, vol. 223, pp. 34–49, Mar. 2019. [Online]. Available: <http://www.sciencedirect.com/science/article/pii/S0034425718305959>
- [21] J. Li, X. Huang, and J. Gong, "Deep neural network for remote-sensing image interpretation: Status and perspectives," *Nat. Sci. Rev.*, vol. 6, no. 6, pp. 1082–1086, May 2019, doi: [10.1093/nsr/nwz058](https://doi.org/10.1093/nsr/nwz058).
- [22] W. P. W. Kwok, W.-S. Tang, and B. L. Kwok, "An introduction to two exotic mangrove species in Hong Kong: Sonneratia Caseolaris and S. Apetala," *Hong Kong Biodiversity*, no. 10, p. 4, Dec. 2005.
- [23] L. Peng, "The characteristics of mangrove wetlands and some ecological engineering questions in China," *Eng. Sci.*, vol. 6, pp. 33–38, May 2003.
- [24] H. Ren *et al.*, "Sonneratia apetala Buch. Ham in the mangrove ecosystems of China: An invasive species or restoration species?" *Ecol. Eng.*, vol. 35, no. 8, pp. 1243–1248, Aug. 2009.
- [25] F. K. K. Wong and T. Fung, "Combining EO-1 hyperion and Envisat ASAR data for mangrove species classification in Mai Po Ramsar Site, Hong Kong," *Int. J. Remote Sens.*, vol. 35, no. 23, pp. 7828–7856, Dec. 2014.
- [26] K. He, X. Zhang, S. Ren, and J. Sun, "Deep residual learning for image recognition," in *Proc. IEEE Conf. Comput. Vis. Pattern Recognit. (CVPR)*, Jun. 2016, pp. 770–778.
- [27] T.-Y. Lin, P. Dollar, R. Girshick, K. He, B. Hariharan, and S. Belongie, "Feature pyramid networks for object detection," in *Proc. IEEE Conf. Comput. Vis. Pattern Recognit. (CVPR)*, vol. 1, Jul. 2017, p. 4.
- [28] S. Ren, K. He, R. Girshick, and J. Sun, "Faster R-CNN: Towards real-time object detection with region proposal networks," *IEEE Trans. Pattern Anal. Mach. Intell.*, vol. 39, no. 6, pp. 1137–1149, Jun. 2017.
- [29] J. Redmon and A. Farhadi, "YOLOv3: An incremental improvement," 2018, *arXiv:1804.02767*. [Online]. Available: <https://arxiv.org/abs/1804.02767>
- [30] P. F. Felzenszwalb, R. B. Girshick, and D. Mcallester, "Cascade object detection with deformable part models," in *Proc. IEEE Comput. Soc. Conf. Comput. Vis. Pattern Recognit.*, Jun. 2010, pp. 2241–2248.
- [31] T.-Y. Lin, P. Goyal, R. Girshick, K. He, and P. Dollar, "Focal loss for dense object detection," in *Proc. ICCV*, 2017, pp. 2980–2988.
- [32] L. Jiao *et al.*, "A survey of deep learning-based object detection," *IEEE Access*, vol. 7, pp. 128837–128868, 2019, doi: [10.1109/ACCESS.2019.2939201](https://doi.org/10.1109/ACCESS.2019.2939201).
- [33] M. Everingham, L. Van Gool, C. K. I. Williams, J. Winn, and A. Zisserman, "The Pascal visual object classes (VOC) challenge," *Int. J. Comput. Vis.*, vol. 88, no. 2, pp. 303–338, Jun. 2010, doi: [10.1007/s11263-009-0275-4](https://doi.org/10.1007/s11263-009-0275-4).
- [34] O. Russakovsky *et al.*, "ImageNet large scale visual recognition challenge," *Int. J. Comput. Vis.*, vol. 115, no. 3, pp. 211–252, Dec. 2015, doi: [10.1007/s11263-015-0816-y](https://doi.org/10.1007/s11263-015-0816-y).
- [35] M. Everingham, S. M. A. Eslami, L. Van Gool, C. K. I. Williams, J. Winn, and A. Zisserman, "The Pascal visual object classes challenge: A retrospective," *Int. J. Comput. Vis.*, vol. 111, no. 1, pp. 98–136, Jan. 2015, doi: [10.1007/s11263-014-0733-5](https://doi.org/10.1007/s11263-014-0733-5).
- [36] P. Henderson and V. Ferrari, "End-to-end training of object class detectors for mean average precision," Jul. 2016, *arXiv:1607.03476*. [Online]. Available: <https://arxiv.org/abs/1607.03476>
- [37] P. Felzenszwalb, D. McAllester, and D. Ramanan, "A discriminatively trained, multiscale, deformable part model," in *Proc. IEEE Conf. Comput. Vis. Pattern Recognit.*, Jun. 2008, pp. 1–8.